Milliwatt-level output power in the sub-terahertz range generated by photomixing in a GaAs photoconductor

Emilien Peytavit, Sylvie Lepilliet, Francis Hindle, Christophe Coinon, Tahsin Akalin, Guillaume Ducournau, Gaël Mouret, Jean-Francois Lampin

Milliwatt-level output power in the sub-terahertz range generated by photomixing in a GaAs photoconductor

Cite as: Appl. Phys. Lett. **99**, 223508 (2011); https://doi.org/10.1063/1.3664635
Submitted: 29 September 2011 • Accepted: 05 November 2011 • Published Online: 29 November 2011

E. Peytavit, S. Lepilliet, F. Hindle, et al.

Milliwatt-level output power in the sub-terahertz range generated by photomixing in a GaAs photoconductor

E. Peytavit,[1,a)] S. Lepilliet,[1] F. Hindle,[2] C. Coinon,[1] T. Akalin,[1] G. Ducournau,[1] G. Mouret,[2] and J.-F. Lampin[1]
[1]*IEMN, UMR CNRS 8520, Université de Lille, 59652 Villeneuve d'Ascq, France*
[2]*LPCA, UMR CNRS 8101, Université du Littoral Côte d'Opale, 59140 Dunkerque, France*

(Received 29 September 2011; accepted 5 November 2011; published online 29 November 2011)

It is shown from accurate on-wafer measurement that continuous wave output powers of 1.2 mW at 50 GHz and 0.35 mW at 305 GHz can be generated by photomixing in a low temperature grown GaAs photoconductor using a metallic mirror Fabry-Pérot cavity. The output power is improved by a factor of about 100 as compared to the previous works on GaAs photomixers. A satisfactory agreement between the theory and the experiment is obtained in considering both the contribution of the holes and the electrons to the total photocurrent. © *2011 American Institute of Physics*. [doi:10.1063/1.3664635]

The so-called terahertz gap is shrinking due to the increase of the maximum oscillation frequency of the InP-based high electron mobility transistor (HEMT), which is now beyond 1 THz and allows to make terahertz monolithic circuits (TMIC), such as low noise amplifiers operating up to 670 GHz.[1] However, this narrowband approach is not well suited for every potential application in the terahertz range. For applications which need tunable continuous-wave sources as the gas spectroscopy, the generation of terahertz waves based on the mixing of two infrared lasers on a photoconductor is a good alternative. The photomixing has been shown for the first time in 1955 with a photocathode illuminated by two Zeeman components of an atomic spectral line separated by 10 GHz.[2] In the 1990s, this technique has been adapted to the terahertz range thanks to an ultrafast photoconductor, consisting of an interdigitated electrode capacitance on a low-temperature-grown GaAs (LT-GaAs) layer[3] and pumped by two Ti:Al_2O_3 lasers. Actually, the LT-GaAs, discovered some years before,[4] seemed to be a perfect semiconductor for ultrafast optoelectronics, due to a subpicosecond carrier lifetime, a high electric-field breakdown (∼300 kV/cm) (Ref. 5) combined with a relatively high electron mobility (∼150 cm^2/Vs).[6] However, since almost twenty years, the output power generated in the millimeter wave and terahertz range by photomixing in a LT-GaAs based photoconductor integrated with a wideband antenna has always been below 10 μW, i.e., ∼10 μW (Refs. 3 and 7) at 100 GHz, 4 μW at 300 GHz,[3,7] and around 1 μW at 800 GHz.[3,7,8] And the best results, i.e., ∼80 μW at 300 GHz and 2.6 μW at 1 THz, have been achieved with InP-based uni-travelling carrier photodiodes (UTC-PD) initially developed for telecom applications and pumped by 1.55-μm-wavelength lasers.[9] Recently, a high dc responsivity (>0.1 A/W) has been measured on a LT-GaAs vertical resonant photoconductor[10] thanks to a metallic mirror Fabry-Pérot cavity and deep submicron electrode spacing resulting in a high carrier and current density. It has been demonstrated that this high dc responsivity, unlike previous works, is almost constant up to the millimeter wave range.[11] In this letter, it is shown by on wafer measurement that the power generated by photomixing in a GaAs photodetector coupled to a 50-Ω-coplanar probe is above 1 mW at 50 GHz and reaches 0.35 mW at 305 GHz. It represents a ∼100-times-improvement as compared to the previous works and is comparable to the power obtained with a UTC-PD integrated with a narrow band matching impedance circuit.[12]

Fig. 1 shows a scanning electron microscope picture of the LT-GaAs resonant photoconductor coupled to a 50-Ω-coplanar waveguide. The LT-GaAs layer of thickness around $w = 0.28$ μm is sandwiched between two gold layers which serve as the same time as bias electrodes and optical mirrors. The diameter of the active photoconductive area is $d = 6$ μm. The upper gold layer is semi-transparent, and a silicon nitride encapsulation and isolation layer is deposited on the photoconductive area. The upper semi-transparent electrode and the background electrodes are linked to a ∼50 Ω coplanar waveguide by air-bridges. The fabrication process of a LT-GaAs photoconductor on a high resistivity silicon substrate is detailed in Refs. 10 and 11.

A schematic overview of the experimental set-up is shown in Fig. 2. A combination of half-wave plates and polarizers is used to ensure that the polarization of the two extended cavity laser diodes (ECLDs) are parallel and have equal powers. The optical beatnote is generated by spatially

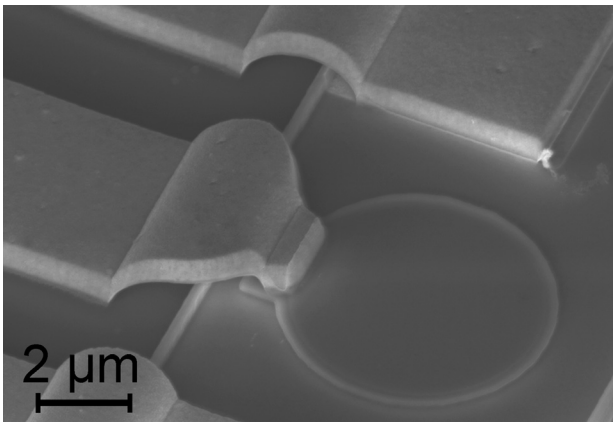

FIG. 1. Scanning electron microscope picture of the resonant LT-GaAs photoconductor.

[a)]Electronic mail: Emilien.peytavit@iemn.univ-lille1.fr.

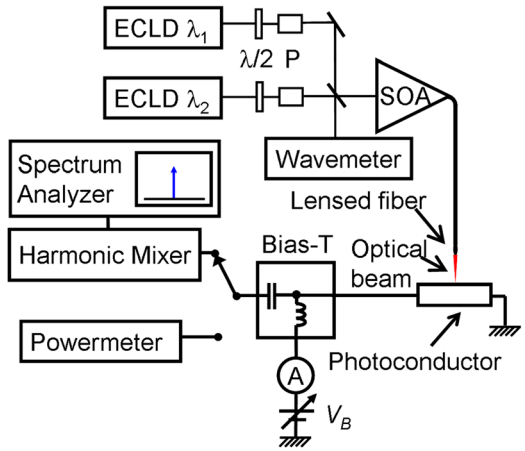

FIG. 2. (Color online) Experimental set-up used for the photomixing experiment: $\lambda/2$, half-wave plate; P, polarizer; SOA, semiconductor optical amplifier.

overlapping the two ECLDs ($\lambda \approx 776\,\mu$m) and used to seed a tapered semiconductor optical amplifier, the output of which is fiber-coupled.[8] The optical wave is then focused into a 4 μm-wide Gaussian spot by a lensed fiber. In the millimeter wave range, the wave generated in the photoconductor at the beat frequency is collected by a 50-GHz coplanar probe and sent to a spectrum analyzer or to a power meter through a 2.4 mm coaxial cable and a 50-GHz bias-T. In the terahertz range, a waveguide 220-325 GHz coplanar probe is used to collect the generated wave and to couple it to a subharmonic mixer driven by the spectrum analyser or to a power meter (Erickson PM4). In both frequency ranges, the losses induced by the coplanar probes, the connectors and the waveguides are measured and are taken into account. They reach 8.65 dB at 50 GHz and 6.4 dB at 305 GHz. Furthermore, in each band, the signal linewidth has been measured and is about 1 MHz for a 20-ms-sweeping time.

Fig. 3 shows the experimental dc photocurrent (I_{dc}) as a function of the bias voltage (V_B) measured on 6-μm-diameter photoconductor for an optical power of 107 mW. As previously reported, I_{dc} curves can be divided in two parts: a first, "high mobility" part related mainly to the electron transport and a "low mobility" part related to the hole transport.[10] In

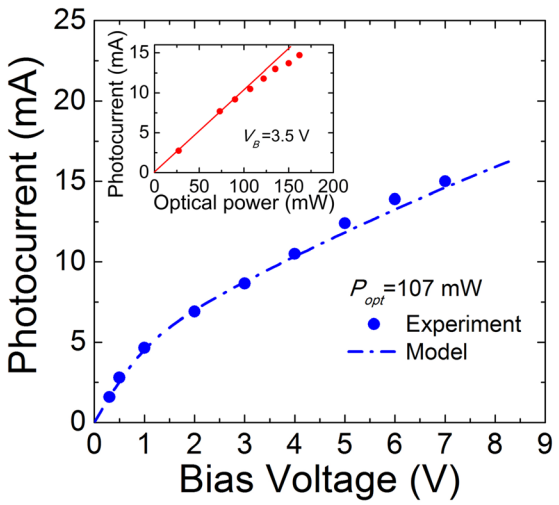

FIG. 3. (Color online) Bias voltage dependence of the dc photocurrent I_{dc} for an optical power $P_{opt} = 107$ mW. Inset: I_{dc} as function of the optical power for a bias voltage $V_B = 3.5$ V.

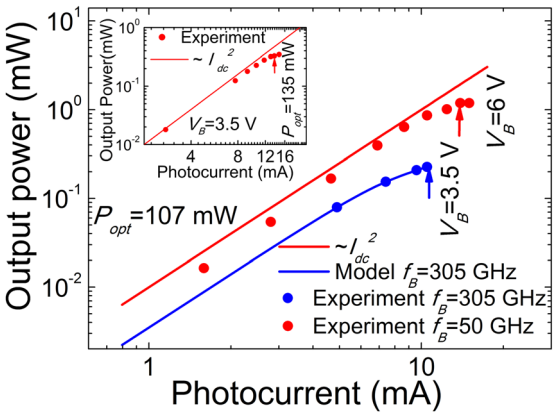

FIG. 4. (Color online) Output power versus photocurrent for beatnotes frequencies $f_B = 50$ and 305 GHz. The optical power ($P_{opt} = 107$ mW) is kept constant while the bias voltage is varied. Inset: output power versus photocurrent for $f_B = 305$ GHz. The bias voltage ($V_B = 3.5$ V) is kept constant while P_{opt} is varied.

the inset of the Fig. 3 is shown the optical power (P_{opt}) dependency of I_{dc} when the bias voltage $V_B = 3.5$ V is kept constant. It can be noticed that a slight saturation effect occurs, which can be related to the increase of the device temperature and the subsequent decrease of the carrier velocity. However, the dc photocurrent reaches 14.7 mA (and a record current density of 50 kA/cm^2 is achieved) at $P_{opt} = 162$ mW corresponding to a very low dc photoresistance $R_0 = 1/G_0 = 238\ \Omega$.

Fig. 4 shows the output power (P_L) versus the photocurrent for an optical power $P_{opt} = 107$ mW kept constant and a varying bias voltage. For $f_B = 50$ GHz, the output power is proportional to the square of the dc photocurrent up to $V_B = 6$ V as it has been previously shown.[11] An output power of ~1.2 mW has been measured for a dc photocurrent of 13.9 mA at the bias voltage saturation $V_B = 6$ V. For $f_B = 305$ GHz, the saturation appears around 3.5 V. In the inset of Fig. 4, the output power is plotted at $f_B = 305$ GHz as a function of I_{dc} when V_B is kept constant and P_{opt} is varied. The output power begins to saturate at $P_{opt} = 135$ mW and reached 0.35 mW at $P_{opt} = 162$ mW.

It seems possible to explain the lower bias voltage saturation at 305 GHz in comparison with 50 GHz in considering electron and holes with different lifetime and mobility. The dc photocurrent in a lifetime-limited photoconductor can be expressed as $I_{dc} = (q/hv)\eta P_{opt}(g_e + g_h)$, where q is the unit electric charge, $\eta = P_{abs}/P_{opt}$ is the quantum efficiency with P_{abs} the optical power absorbed in the LT-GaAs layer, $g_{e(h)} = \tau_{e(h)}/\tau_{tre(h)}$ is the electron (hole) optical gain, and $\tau_{tre(h)} = w/v_{e(h)}$ the electron (hole) transit time. In order to make a basic model of the dc photocurrent as a function of the bias voltage, we make three assumptions: (1) the electric field and the carrier density are assumed to be homogeneous across the layer, (2) space charge effects are negligible, and (3) the electron and holes have similar electric field (E) dependencies of their velocity, which is used in standard GaAs only for holes,[13]

$$v_{e(h)} = \frac{\mu_{e(h)}E}{\left(1 + \left(\frac{\mu_{e(h)}E}{vs_{e(h)}}\right)^{\beta}\right)^{1/\beta}}, \quad (1)$$

with $vs_e \approx vs_h \approx 0.6 \times 10^7$ cm/s.[14] Monte-Carlo simulations in compensated GaAs have indeed shown that the electron peak velocity almost disappears for high doping compensation.[14] In the following paragraphs, it is assumed that $\mu_e = 150$ cm^2/Vs, $\mu_h = 10$ cm^2/Vs, $\tau_e = 0.5$ ps, and $\tau_h = 3$ ps. The electron lifetime in the LT-GaAs layer was measured by time-resolved photoreflectance.[10] The hole lifetime is very difficult to measure, but the attempts already done have shown that it is likely to reach a few picoseconds.[15,16] In Fig. 3, the calculated I_{dc} is plotted as a function of V_B for $P_{opt} = 107$ mW with $\eta = 0.58$ and $\beta = 2.4$, which were both used as fit parameters. A good agreement is achieved between the model and the experimental data which seems to confirm the assumptions. However, it is only a phenomenological model, and a physical model which takes into account of all the complexity of the device is well beyond the scope of this letter.[17]

Concerning the output power, the behaviour as a function of the optical power and the bias voltage requires an electrical model of the circuit. In a photomixing experiment, in which two equal power laser beams with parallel polarization of frequency offset f_B strike a photoconductor, the optical incident power can be expressed as $P(t) = P_{opt}(1 + \cos(\omega_B t))$, where $\omega_B = 2\pi f_B$ and $P_{opt}/2$ is the optical power of each beam. It can be shown[18] in assuming that the higher harmonics are negligible that the photoconductor can be modelled as an ac current source of magnitude I_{ac} and phase ϕ with an internal admittance consisting of its dc photoconductance $G_0 = I_{dc}/V_B$ shunted by the capacitance (C) of the photoconductor. In the present case, a capacitance of 13 fF was extracted from a 3D electromagnetic simulation. I_{ac} and ϕ can be expressed in a lifetime limited photoconductor as follows:

$$I_{ac} = \frac{I_{dc}}{\sqrt{1 + (\omega_B \tau)^2}} \quad \text{and} \quad \phi = \tan^{-1}(\omega_B \tau), \tag{2}$$

where τ is the carrier lifetime of the photoconductor. To take into account separately electron and hole photocurrents, we consider in our case two current sources: an electron current source I_{ace} and a hole current source I_{ach} which are linked to I_{dce} and I_{dch} by the Eq. (2) with $\tau = \tau_{e(h)}$. The two resulting ac current sources can be replaced by an equivalent ac source

$$I_{aceq} = \sqrt{I_{ace}^2 + I_{ach}^2 + 2 I_{ace} I_{ach} \cos(\phi_h - \phi_e)}. \tag{3}$$

Then the power dissipated in a load of admittance $Y_L = G_L + jB$ (or impedance $Z_L = 1/Y_L = R_L + jX_L$) with $j^2 = -1$ is

$$P_L = \frac{1}{2} \frac{I_{aceq}^2 G_L}{|G_L + G_0 + j(\omega_B C + B)|^2}. \tag{4}$$

And the maximum power (P_{Lmax}) is achieved at the perfect matching condition when $Y_L = Y_s^*$ or $Z_L = Z_s^*$ with $Y_S = G_0 + j\omega_B C$ ($Z_s = 1/Y_s$), the source admittance (impedance), and can be expressed as $P_{Lmax} = I_{aceq}^2/8G_0$. In the present experiment, the perfect matching condition is not achieved but R_0 is 40 times lower than in the case of standard planar LT-GaAs photomixers ($R_0 \approx 8$ kΩ),[19] which explain the dramatic improvement in output power.

Finally, in order to calculate the output power as a function of the bias voltage or the dc photocurrent, it appears from the Eq. (4) that Z_L must be precisely known. In the case of an on-wafer-measurement with coplanar probes followed by a perfectly matched powermeter, Z_L is directly related to the impedance mismatch, i.e., the reflection coefficient ρ, between the probe and the 50-Ω coplanar waveguide. Its magnitude can be easily determined but its phase is very difficult to quantify at 300 GHz. A magnitude of −10.4 dB was measured by the probe manufacturer, which gives for Z_L (Y_L) a set of possible values. Fig. 4 shows the output power calculated by Eq. (4) with $Z_L = 28 + j12$ Ω, which gives the best fit with the experimental output power. The maximum power at 305 GHz (at $P_{opt} = 162$ mW and $V_B = 3.5$ V) is achieved with a total dissipated power $P_{tot} \approx (1 - \Re) \times P_{opt} + V_B \times I_{dc} = 0.18$ W, with an estimated optical reflection coefficient $\Re = 0.2$. The efficiency at 305 GHz is $\eta_{tot} = P_L/P_{tot} = 0.2$ % which is comparable to narrow band electronic sources. It should be noticed that there was no active cooling which could be likely to improve the saturation power. An output power of 60 μW at 600 GHz and 13 μW at 1 THz is expected from this model for a load of impedance $Z_L = 25$ Ω. A maximum power of 150 μW in a narrow band around 1 THz could be achieved with a perfectly matched load impedance.

This work has been supported by the CNRS, the Lille1 University and the "Région Nord Pas de Calais."

[1] W. R. Deal, X. B. Mei, K. M. K. H. Leong, V. Radisic, S. Sarkozy, and R. Lai, IEEE Trans. Terahertz Sci. Technol. **1**, 25 (2011).
[2] A. T. Forrester, R. A. Gudmundsen, and P. O. Johnson, Phys. Rev. **99**, 1691 (1955).
[3] E. R. Brown, K. A. McIntosh, K. B. Nichols, and C. L. Dennis, Appl. Phys. Lett. **66**, 285 (1995).
[4] F. W. Smith, A. R. Calawa, C. L. Chen, M. J. Manfra, and L. J. Mahoney, IEEE Trans. Electron Devices **34**, 2375 (1987).
[5] F. W. Smith, H. Q. Le, V. Diadiuk, M. A. Hollis, A. R. Calawa, S. Gupta, M. Frankel, D. R. Dykaar, G. A. Mourou, and T. Y. Hsiang, Appl. Phys. Lett. **54**, 890 (1989).
[6] S. Gupta, M. Y. Frankel, J. A. Valdmanis, J. F. Whitaker, G. A. Mourou, F. W. Smith, and A. R. Calawa, Appl. Phys. Lett. **59**, 3276 (1991).
[7] M. Mikulics, E. A. Michael, R. Schieder, J. Stutzki, R. Gusten, M. Marso, A. V. D. Hart, H. P. Bochem, H. Luth, and P. Kordos, Appl. Phys. Lett. **88**, 041118 (2006).
[8] E. Peytavit, A. Beck, T. Akalin, J.-F. Lampin, F. Hindle, C. Yang, and G. Mouret, Appl. Phys. Lett. **93**, 111108 (2008).
[9] H. Ito, F. Nakajima, T. Furuta, K. Yoshino, Y. Hirota, and T. Ishibashi, Electron. Lett. **39**, 1828 (2003).
[10] E. Peytavit, C. Coinon, and J.-F. Lampin, J. Appl. Phys. **109**, 016101 (2011).
[11] E. Peytavit, C. Coinon, and J.-F. Lampin, Appl. Phys. Express **4**, 104101 (2011).
[12] H. Ito, T. Furuta, Y. Muramoto, T. Ito, and T. Ishibashi, Electron. Lett. **42**, 1424 (2006).
[13] Z. M. Li, K. M. Dzurko, A. Delage, and S. P. McAlister, IEEE J. Quantum Electron. **28**, 792 (1992).
[14] E. Y. Wu and B. H. Yu, Appl. Phys. Lett. **58**, 1503 (1991).
[15] R. Adomavicius, A. Krotkus, K. Bertulis, V. Sirutkaitis, R. Butkus, and A. Piskarskas, Appl. Phys. Lett. **83**, 5304 (2003).
[16] T. S. Sosnowski, T. B. Norris, H. H. Wang, P. Grenier, J. F. Whitaker, and C. Y. Sung, Appl. Phys. Lett. **70**, 3245 (1997).
[17] M. Goodman and A. Rose, J. Appl. Phys. **42**, 2823 (1971).
[18] P. D. Coleman, R. C. Eden, and J. N. Weaver, IEEE Trans. Electron Devices **11**, 488 (1964).
[19] S. M. Duffy, S. Verghese, and K. A. McIntosh, *Sensing with Terahertz Radiation*, edited by D. Mittelman (Springer, Berlin, 2003) p. 193.